

Polypyrrole actuators: modeling and performance

John D.W. Madden*, Peter G.A. Madden and Ian W. Hunter
Massachusetts Institute of Technology, Cambridge MA 02139

ABSTRACT

Conducting polymer actuators generate forces that exceed those of mammalian skeletal muscle by up to two orders of magnitude for a given cross-sectional area, require only a few volts to operate, and are low in cost. However application of conducting polymer actuators is hampered by the lack of a full description of the relationship between load, displacement, voltage and current. In an effort to provide such a model, system identification techniques are employed. Stress-strain tests are performed at constant applied potential to determine polypyrrole stiffness. The admittance transfer function of polypyrrole and the associated electrolyte is measured over the potential range in which polypyrrole is highly conductive. The admittance is well described by treating the polymer as a volumetric capacitance of $8 \cdot 10^7 \text{ F} \cdot \text{m}^{-3}$ whose charging rate is limited by electrolyte resistance and diffusion within polypyrrole. The relationship between strain and charge is investigated, showing that strain is directly proportional to charge via the strain to charge density ratio, $\alpha = 1 \cdot 10^{-10} \text{ m}^3 \cdot \text{C}^{-1}$, at loads of up to 4 MPa. Beyond 4 MPa the strain to charge ratio is time dependent. The admittance models, stress/strain relation and strain to charge relationship are combined to form a full description of polypyrrole electromechanical response. This description predicts that large increases in strain rate and power are obtained through miniaturization, yielding bandwidths in excess of 10 kHz. The model also enables motor designers to optimize polypyrrole actuator geometries for their applications.

1. INTRODUCTION

Conducting polymer actuators are rapidly being advanced from promising laboratory phenomena¹⁻⁸ towards full-fledged engineering materials^{9,10}. Most studies to date have investigated the contractile properties of either of two conducting polymers, polypyrrole or polyaniline. This paper summarizes observations made in the course of studying electrochemically driven polypyrrole actuators. Key properties are measured and modeled including the relationships between voltage, current, stress, strain, power, and efficiency. The measurements and models enable device designers to predict and optimize actuator behavior, and help reveal the potential and limitations of conducting polymer actuators. The system identification approach employed to measure, describe and predict the behavior of polypyrrole actuators should prove useful to investigators of other actuator technologies.

1.1. Background

Conducting polymers are an unusual class of organic materials that exhibit high electronic conductivities¹¹. Conductivities can match copper at $6 \cdot 10^7 \text{ S} \cdot \text{m}^{-1}$, but are more typically three or more orders of magnitude lower in air stable materials. Common to all conducting polymers is a conjugated backbone. Oxidation or reduction creates delocalized charge carriers along the backbone. Changes in oxidation state are generally performed chemically or electrochemically, and can lead to conductivity variations of 13 orders of magnitude, an effect that is made use of in polymer transistors¹².

During electrochemical oxidation, charge is removed from the polymer backbone. Ions from a surrounding electrolyte enter or leave the polymer, serving to maintain charge balance. In the process of changing oxidation state, conductivity, optical absorption, permeability, hydrophobicity and stored charge all change in a controllable manner, enabling transistors, filters, capacitors, and batteries, among other devices, to be constructed¹¹. Dimensional changes also accompany shifts in oxidation state, suggesting the use of conducting polymers as actuators.

The dimensional changes are attributed in varying degrees to conformational changes, solvent insertion, ion insertion and electrostatic interactions¹. In polypyrrole expansion rate is correlated with ion flux into the polymer, and appears to be related to ion size¹³. The magnitude of the volume change per unit charge corresponds closely with the volume of the inserted charge^{10,14}. In general volume changes and linear strains are proportional to the charge transferred^{1,2,5,10,14-16}. High current corresponds to large strain rate and power.

* jmadden@mit.edu; <http://bioinstrumentation.mit.edu>.

Conducting polymer actuators are of technological interest due to their low operating voltages, high forces, moderate strains, controllability and low cost. The operating voltage range is typically less than 1 V, with short bursts of up to 10 V being used to increase power¹⁷. Such voltages are readily provided by batteries and are of particular value in micro-machined devices¹⁸, which currently incorporate high voltage activated piezoelectric and electrostatic actuators. The fact that displacement is proportional to charge transfer in conducting polymer actuators makes them relatively easy to control, an advantage over shape memory alloys¹⁹. Unlike mammalian muscle and electromagnetic motors, conducting polymers do not expend significant energy when holding a load in place, greatly reducing losses in static applications such as switches and valves. Forces exceed the 350 kN·m⁻² of mammalian skeletal muscle¹⁷ by up to two orders of magnitude¹⁰. The power to mass is at the low end of the 20-200 W·kg⁻¹ found in mammalian skeletal muscle, and promises to greatly exceed muscle.

Conducting polymer actuators have yet to be fully characterized. Reports of actuator efficiency are sparse^{1,10,14,20,21}. Models of actuator response are being developed^{9,21}, but these have yet to fully describe the relationship between input electrical energy and mechanical output. This paper focuses on the identification and modeling of polypyrrole actuator response, culminating in a description of the electromechanical properties including electrical to mechanical conversion efficiency. Work remains to be done to describe the effects of cycling and storage on actuator response.

The methods and results presented here depart from previous work in a number of ways. A low temperature, non-aqueous electrodeposition method is employed to synthesize polypyrrole²². This is done to increase conductivity and improve mechanical properties, thereby minimizing dissipation and maximizing force. Furthermore, the polypyrrole oxidation state is maintained within a potential range in which it is highly conductive. The continually high conductivity allows the active properties of relatively long freestanding films to be measured and analyzed without concern about potential drops across the films produced by input currents. This approach does not sacrifice the magnitude of strain that can be obtained from the polymer¹⁰. Finally, polymer electrochemical and electromechanical response is investigated using swept sine techniques, as opposed to the step and ramp inputs that have previously been employed^{9,14,16,23}. The resulting frequency response enables transport mechanisms and time-dependent behaviors to be readily identified and modeled. This methodology also allows the influence of electrical stimulus on mechanical response to be distinguished from load and displacement induced creep and relaxation.

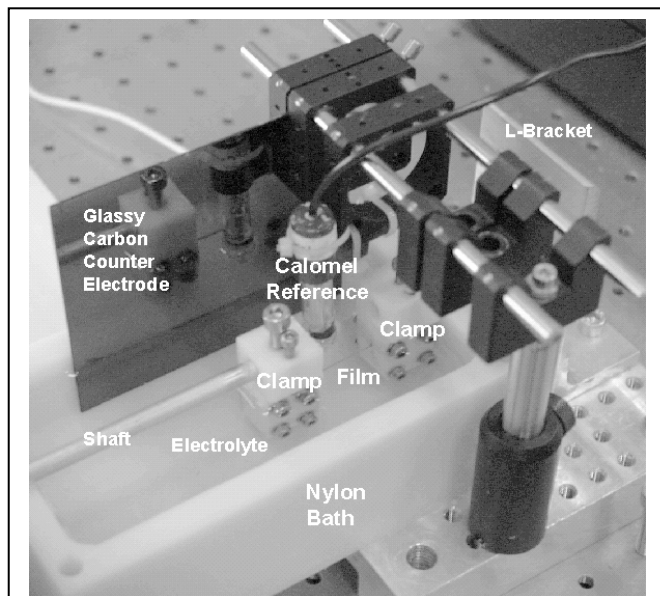


Figure 1: A view of the electromechanical test cell, showing the positioning of the clamps, the reference electrode and the film. A second identical counter electrode on the near side of the film has been removed. A load cell measures force between the rightmost clamp and the fixed L-bracket.

2. POLYMER SYNTHESIS

The method of polypyrrole synthesis follows the procedure of Yamaura and colleagues²². Polypyrrole is chosen for a number of reasons. Pei²⁴ and Smela²⁵ showed that large cantilever deflections are obtained using polypyrrole. Early experiments also showed that rapid deflections are possible⁸. Further experimentation demonstrated that strains of 2 % are obtainable at stresses of 5 MPa or greater¹⁴. Polypyrrole also exhibits the highest conductivity of any intrinsically conducting polymer studied to date apart from polyacetylene. High conductivity is advantageous, as it enables films and fibers to be electrochemically activated without concern for potential drops, which reduce efficiency and can cause activation to be non-uniform.

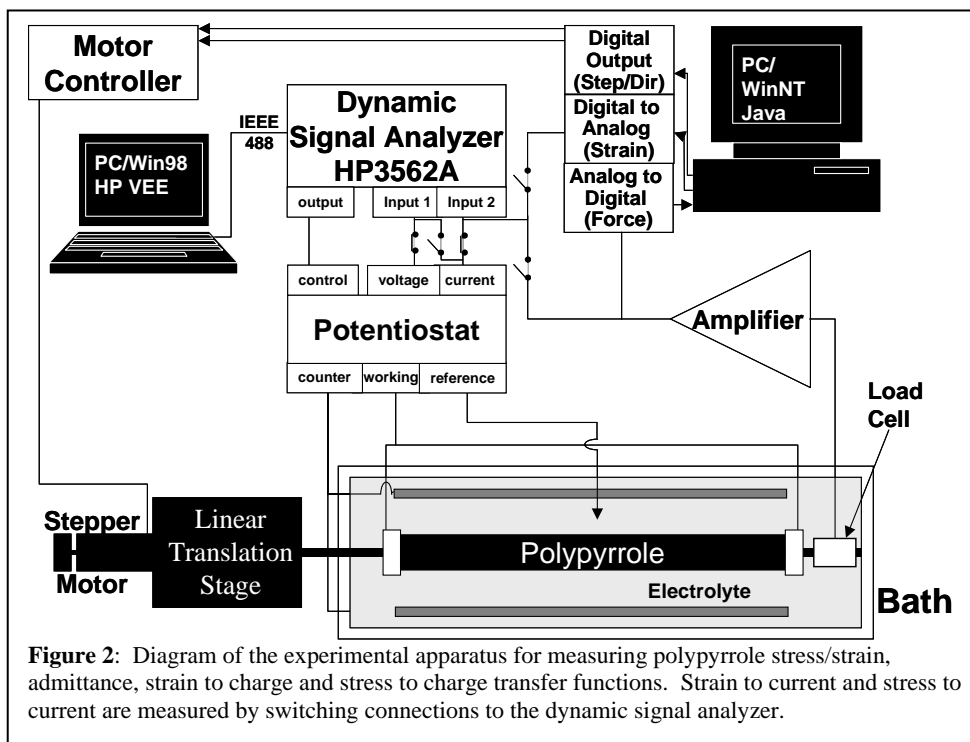
Films are grown from a solution of 0.06 M freshly distilled pyrrole monomer (Aldrich, www.aldrich.com) and 0.05 M (C₂H₅)₄PF₆ (tetraethylammonium hexafluorophosphate, Aldrich) in propylene carbonate¹⁰. Polypyrrole is deposited on to polished glassy carbon substrates (Alfa Aesar, www.alfa-aesar.com) at current densities of between 1 and 2 A·m⁻², resulting in film thickness of between 8 and 52 μm.

The counter electrode is copper. Deposition takes place at temperatures between -30 °C and -45 °C in a nitrogen-saturated solution. The resulting films have conductivities of between 20 and 45 kS·m⁻¹, densities of 1500 to 1800 kg·m⁻³ dry and tensile strengths of 30 to 50 MPa. The polished glassy carbon substrates take the form of either 100 mm × 100 mm × 1 mm

thick slabs, or of 85 mm tall and 72 mm diameter crucibles. Crucibles are employed to obtain films that are up to 1.5 m in length, and 4 mm wide.

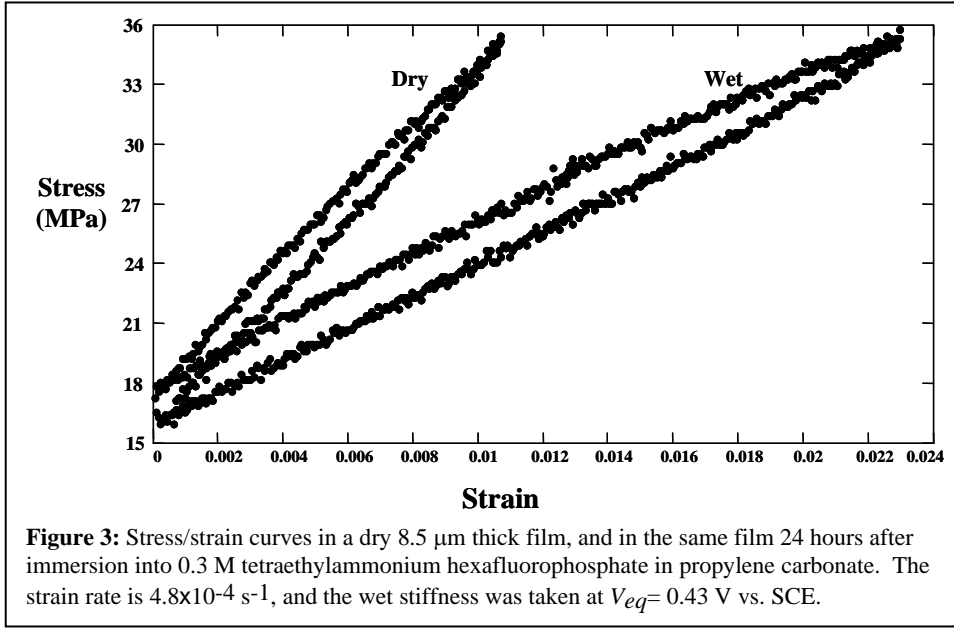
X-ray diffraction analysis reveals that the material is ~50% crystalline, containing ordered regions that are ~2 nm across²⁶⁻²⁸. Polymer electrical resistance merely doubles¹⁰ between room temperature and 6 K, demonstrating nearly metallic behavior¹¹. Based on the x-ray and conductivity data, it has been suggested that the structure is inhomogeneous, containing ordered conductive, crystalline and disordered regions with incoherent chain orientation²⁹.

Elemental analyses show that dry films have an oxidation state of between 0.3 and 0.4 charges per monomer as grown. Films are dried by baking under vacuum or in a nitrogen environment at between 90 °C and 100 °C. The elemental analyses are performed by Galbraith Laboratories, Knoxville Tennessee, and agree with the range of oxidation levels reported by Yamaura^{22,30-32}. When soaked in propylene carbonate, the solvent comprises 40-50 % of the total mass. Thermal gravimetric analysis combined with mass spectroscopy and, separately, infra-red absorption spectroscopy, indicate that the polypyrrole backbone does not thermally degrade appreciably under nitrogen until 375 °C.



3. EXPERIMENTAL APPARATUS AND METHODS

Later sections present stress/strain relationships, polymer admittance plots, and data relating stress, strain and charge. Measurements are made on polypyrrole films that are clamped at either end and immersed in an electrolyte filled bath. The bath is shown in Figure 1, and a schematic of the entire apparatus is depicted in Figure 2. The electrolyte consists of tetraethylammonium hexafluorophosphate salt dissolved in propylene carbonate at concentrations of 0.3 M or 0.37 M. The bath is both an electrochemical cell and mechanical test bed. The polypyrrole film provides the working electrode of the cell, and is electrically contacted at both ends. The films employed are 50 or 80 mm long, 3 to 5 mm wide and 8.5 or 12.5 μm thick. Two 100 mm × 100 mm glassy carbon plates (Alfa Aesar), one of which is shown in Figure 1, serve as counter electrodes. They are placed at either edge of the bath, 65 mm apart, equidistant from the clamped film, and with their bases resting at the bottom of the bath and immersed in 35 mm of electrolyte. Both saturated calomel reference electrodes and non-aqueous Ag/AgClO₄ reference electrodes (Bioanalytical Systems MF-2062, www.bioanalytical.com) are employed. The Ag/AgClO₄ reference electrodes are filled with 0.01 M AgClO₄ (Aldrich) and 0.05 M (C₂H₅)₄NPF₆ following the methods of Courtot-Coupez and L'Her³³. The Ag/AgClO₄ electrodes are found to have potentials of 0.716 V vs. standard calomel at 20 °C. The polymer to counter electrode potential is controlled using a custom voltage feedback circuit (potentiostat)¹⁰, which applies the sum of an equilibrium potential and a swept sine input. The equilibrium potential is under computer control via digital to analog output (National Instruments PCI-MIO16XE-10, www.ni.com). A 0.1 mHz to 100 kHz swept sine input is generated by a dynamic signal analyzer (DSA, Hewlett Packard HP3562A, www.agilent.com). Voltage and current are input to the DSA in measuring admittance, current and strain are input during strain to current transfer function measurements, and stress and current are input during stress to current transfer function measurements. A stepper motor (Compumotor 57-51-MO, www.compumotor.com) driven linear stage (NEAT LM-50, www.neat.com) is employed to displace one end of the clamped film. Displacement is under computer control. The computer control allows strain to be ramped, as required during



stress/strain measurements, and enables constant force to be maintained when isotonic conditions are specified. The force feedback required to maintain isotonic conditions is provided by a load cell (Omega LCFD1KG, www.omega.com), whose output is amplified (Vishay Model 2311, www.vishay.com) and digitally sampled. Further description and characterization of the apparatus are provided by Madden¹⁰.

In the experiments presented, the conducting polymer is held in a potential range over which conductivity is high and nearly constant^{10,34}. The cell geometry

is arranged such that electrolyte resistance is much larger than resistive drops across the film. This ensures that the entire polymer is always at a uniform potential.

4. PASSIVE MECHANICAL PROPERTIES

This section summarizes the mechanical properties of polypyrrole in the absence of electrical or chemical stimuli. Tensile strength typically exceeds 50 MPa. Figure 3 shows the stress/strain response of a dry[†] film and one that has been soaked in a

0.3 M (C₂H₅)₄PF₆ propylene carbonate solution. Note that the stiffness halves upon immersion in the electrolyte. Soaking also leads to a 14 % strain and a 25 % increase in mass over the first 8 hours. The decrease in stiffness suggests that polypyrrole is being plasticized by the solvent, which likely forms hydrogen bonds with the polypyrrole backbone. In Figure 4 stress vs. time data are shown for the same wet film strained at three different rates. A standard viscoelastic model, consisting of an elastic stiffness E₁, in series with a parallel elastic element, E₂, and viscous element, η, provides a good description of polypyrrole stress/strain behavior over the timescales shown. The standard model stiffness transfer function, S(s) is:

$$S(s) = \frac{\sigma}{\varepsilon} = \frac{E_1 \cdot (E_2 + \eta \cdot s)}{E_1 + E_2 + \eta \cdot s}, (1)$$

where s is the Laplace variable. For

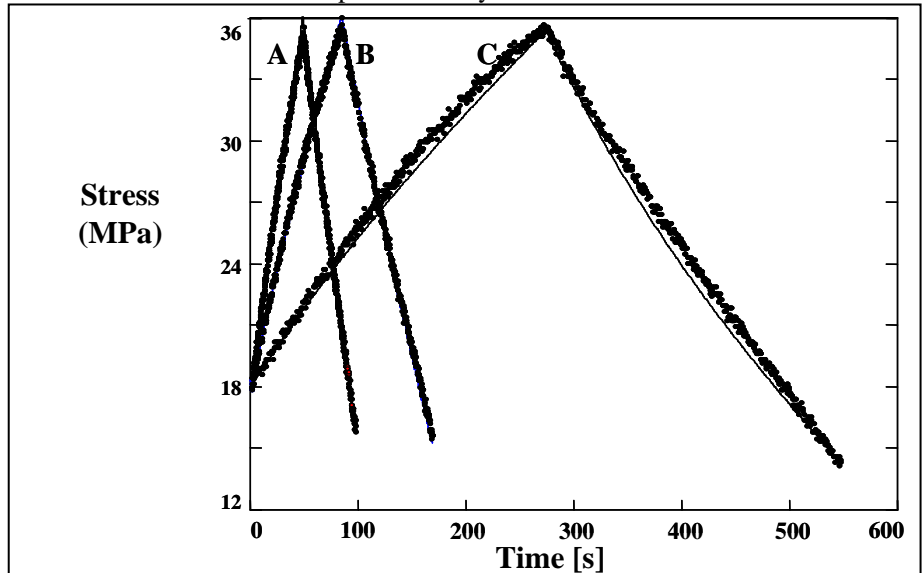
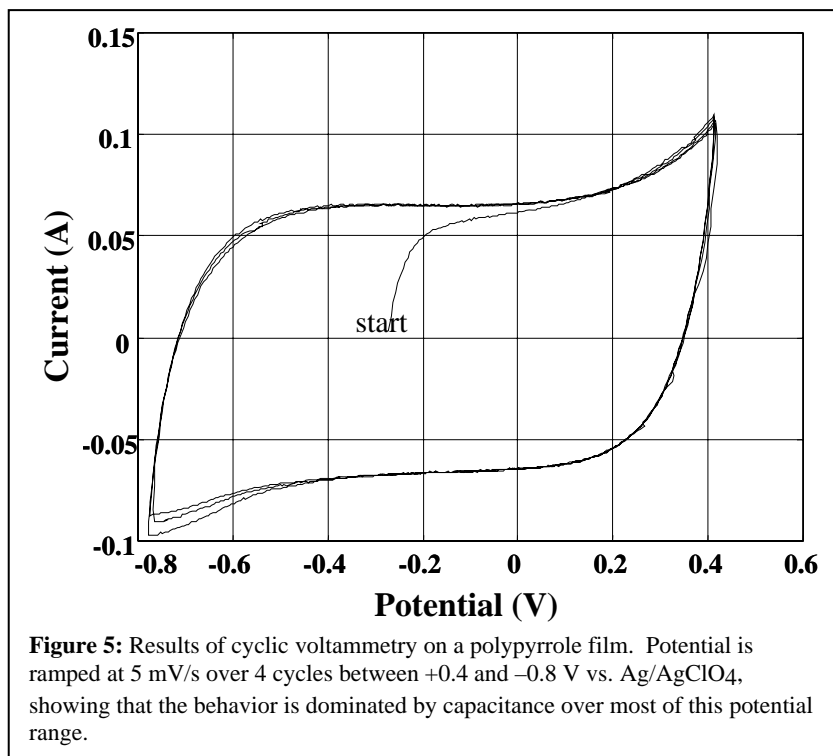


Figure 4: Stress vs. time curves from an 8.5 μm thick film immersed in 0.3 M tetraethylammonium hexafluorophosphate in propylene carbonate and held at V_{eq}= 0.43 V vs. SCE. Strain rates are 4.8x10⁻⁴ s⁻¹ (A), 2.8x10⁻⁴ s⁻¹ (B), and 0.98x10⁻⁴ s⁻¹ (C). A visco-elastic model (solid lines) has been fitted to the data, suggesting linear response over the range of time scales investigated. The model parameters have values of E₁=0.83 MPa, E₂= 1.1 GPa, and b=300 GPa·s.

[†] The 'dry' film contains a residual 20 % solvent by mass as determined by thermal gravimetric analysis¹⁰.

the film soaked in propylene carbonate $E_1=0.83$ GPa, $E_2=1.1$ GPa and $\eta=300$ GPa·s.



Stress/strain behavior is independent of potential between -0.66 to +0.14 V vs. Ag/AgClO₄. The conductivity is also constant over this potential range. The polymer exhibits piezo-resistive behavior however, with a gage factor of 5.0¹⁰. The gage factor and strain range are large compared to metal foil gages. The use of polypyrrole strain gages for force and displacement feedback is currently under investigation.

5. ELECTROCHEMICAL PROPERTIES

Conducting polymer actuators are generally activated electrochemically. Study of the electrochemistry helps determine the kinetics and thermodynamics that govern the transfer of electrical energy to or from the polymer, which in turn impact on actuator power density and electro-mechanical efficiency. This section summarizes the results obtained by measuring admittance[‡] between the reference electrode and polypyrrole films

held under isotonic conditions¹⁰. The data confirm the work of a number of groups³⁵⁻³⁷ demonstrating that at low frequencies polypyrrole and polyaniline behave primarily as capacitors when in their conductive states. Most of the electrical energy input is stored rather than dissipated. Dissipation is the result of electrolyte resistance and the diffusion of dopants within the polymer. Diffusion and RC charging limit the rate of charge transfer to the polymer. Strain is proportional to charge, as shown in Section 6, and therefore these mechanisms also limit strain rate and power. A model is proposed that describes the capacitive thermodynamics, electrolyte resistance and ionic diffusion.

5.1. Voltammetry and polypyrrole capacitance

The electrochemistry of conducting polymers is made complex by the large changes in conductivity, hydrophobicity, solvent content, charge density and permeability that occur as oxidation state is altered. However, there is a wide potential range over which polypyrrole, polyaniline and other conducting polymers behave as capacitors, as demonstrated in polypyrrole by the current measured in response to triangular wave voltage input (voltammogram) in Figure 5. The flat current response between -0.65 V and +0.35 V vs. Ag/AgClO₄ suggests that the thermodynamics of polypyrrole charging are capacitive. The capacitance is 5·10⁴ F·kg⁻¹, independent of surface area, and seven orders of magnitude higher than in polyester capacitors. The conductivity of polypyrrole is high and nearly constant over the same potential range^{10,34}. Note that charging is not instantaneous, as is clear from the rise times at left and right extremes of the sweep. Conducting polymer actuator strain is proportional to the extent of charge transfer, and therefore it is important to understand the origin of the charging time.

5.2. Frequency response

The mechanisms of charging are more clearly identified in the frequency domain. Figure 6 shows the measured admittance transfer function of polypyrrole. The admittance is found to be independent of sinusoidal amplitude up to ±0.5 V, suggesting that a linear model is appropriate and that non-linear mechanisms such as electron exchange kinetics and Nernstian thermodynamics are insignificant in determining the response¹⁰. At high frequencies the admittance matches that of the electrolyte, while at low frequencies the capacitive response is evident. The intermediate frequency behavior is attributed to mass transport of dopants within the polymer³⁵⁻³⁷.

[‡] The admittance is the inverse of the electrical impedance.

A number of mass transport mechanisms have been proposed, all of which are described by a linear diffusion model^{9,10,35-37}. The capacitance has also been attributed to a number of sources, including double layer charging of electrolyte filled pores within the polymer³⁵⁻³⁷, quasi-Nernstian behavior³⁸, and extension of the double layer charging into the bulk material¹⁰. Thus the predicted form of the frequency dependence of admittance is essentially independent of the mechanisms chosen.

Combining the effects of diffusion, capacitance and electrolyte resistance leads to an admittance transfer function, $Y(s)$, of:

$$Y(s) \cdot R = s \cdot \frac{\frac{\sqrt{D}}{\delta} \cdot \tanh\left(\frac{a}{2} \cdot \sqrt{\frac{s}{D}}\right) + \sqrt{s}}{\frac{\sqrt{s}}{R \cdot C} + s^{3/2} + \frac{\sqrt{D}}{\delta} \cdot s \cdot \tanh\left(\frac{a}{2} \cdot \sqrt{\frac{s}{D}}\right)}, \quad (2)$$

where R represents solution resistance, D is the diffusion coefficient, C is double layer capacitance, a is film thickness, δ is the double layer thickness at the electrolyte/polymer interface, and s is the Laplace variable. Details of the derivation are provided by Madden¹⁰. This admittance model is appropriate for films that are very wide and long compared to their thickness, and into which ions can penetrate from two sides⁸. The polymer resistance is assumed to be negligible compared to the electrolyte resistance. As expected the model predicts that at high frequencies ($\text{Im}(s) \rightarrow \infty$), the admittance becomes R^{-1} , and that at low frequencies,

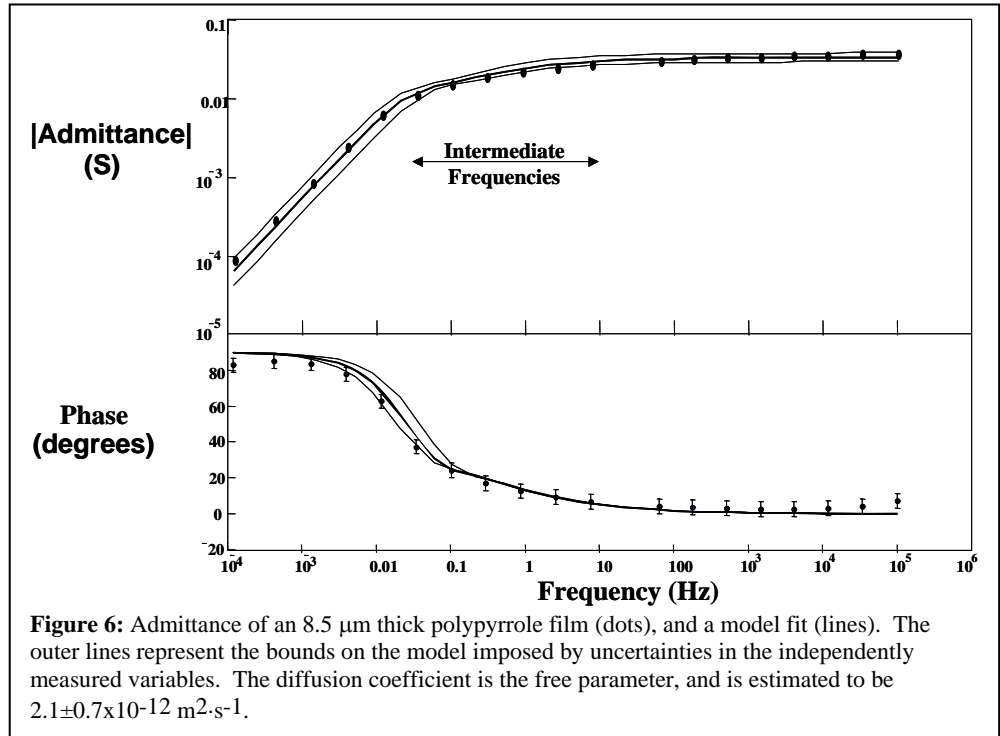
$$Y(s) = s \cdot C \cdot \left(\frac{a}{2 \cdot \delta} + 1\right) = s \cdot C_V, \quad (3)$$

where C_V is the capacitance attributed to the entire polymer volume.

Electrolyte resistance, R , and film thickness, a , are readily measured. The double layer capacitance, C , may be measured, fit, or an accepted value can be used³⁹. The double layer thickness, δ , may be estimated from the capacitance and area, A , assuming a Helmholtz model,

$$\delta = \frac{k \cdot \epsilon_o \cdot A}{C}, \quad (4)$$

where k is the dielectric constant and ϵ_o is the permittivity of free space. The Helmholtz or parallel plate model of double layer capacitance generally applies for electrolyte concentrations above 0.1 M in high dielectric solvents such as water and propylene carbonate³⁹. The diffusion coefficient may be fitted or measured. Methods of independent measurement include radiolabeling and NMR. The lines in Figure 6 show a model fitted to the measured frequency response¹⁰. The diffusion coefficient is estimated from the fit to be $2.1 \pm 0.7 \times 10^{-12} \text{ m}^2 \cdot \text{s}^{-1}$, which is consistent with estimates in the literature¹⁰.



⁸ If ions only penetrate from one side, replace thickness a with $2 \cdot a$ and divide the double layer capacitance, C , by 2 to reflect the change in polymer to electrolyte surface area.

5.3. Factors influencing charging rate

The model suggests two time constants that are particularly relevant to actuator design. The diffusion time constant,

$$\tau_D = \frac{a^2}{4 \cdot D}, \quad (5)$$

represents the time taken to complete diffusion of ions into the polymer. Decreasing film thickness by one order of magnitude increases rate by two orders of magnitude. Increasing the diffusion coefficient, D , also improves response time. This might be achieved by using smaller ions and by modifying the synthesis conditions to make the polymer more porous. If solution resistance is large or the film thickness is small then RC charging may be rate limiting, where the charging time constant is expressed as,

$$\tau_{RCV} = R \cdot C_V. \quad (6)$$

These two time constants suggest that rate is maximized by minimizing film thickness, electrolyte resistance and polymer volume.

Employing resistance compensation can circumvent the RC time constants, leaving diffusion as the rate limiting mechanism. Resistance compensation¹⁷ has enabled the highest reported strain rates, $3 \% \cdot s^{-1}$, and power to mass ratios, $39 \text{ W} \cdot \text{kg}^{-1}$. These are obtained from a $40 \mu\text{m}$ thick film. A 10 nm thick conducting polymer film, approximately the thinnest coherent film that can be anticipated, is expected to respond $10^7 \times$ faster. Assuming a diffusion coefficient of $D=2 \cdot 10^{-12} \text{ m}^2 \cdot \text{s}^{-1}$, such a film is predicted to fully charge in $50 \mu\text{s}$. Similar response times have already been demonstrated in polyaniline transistors and electrochromic devices^{12,40,41}. These fast responses clearly suggest that conducting polymer actuators are promising candidates for micro and nano-mechanical systems, as is being investigated by Smela, Jager and their colleagues⁴².

5.4. Electrical energy storage and dissipation

At frequencies that are higher than both the characteristic diffusion frequency, τ_D^{-1} , and the RC charging frequency, τ_{RCV}^{-1} , dissipation is significant. Efficiency is clearly maximized by operating below these frequencies. Some loss mechanisms are still present at low frequencies however, as demonstrated by the phase in Figure 6, which reaches a maximum of 85 deg , or equivalently an 8% loss. Further investigation is required to determine the origins of the losses, part of which is due to end effects** and electrolyte reactions¹⁰.

5.5. Summary

In its conductive state polypyrrole behaves electrochemically as a capacitor. The enormous capacitance suggests employing polypyrrole for local energy storage as well as actuation. The charging rate is primarily constrained by the RC charging time and by mass transport within polypyrrole. The RC charging time constant is overcome by employing resistance compensation or by reducing electrolyte resistance. Mass transport times are predicted to decrease as the square of film

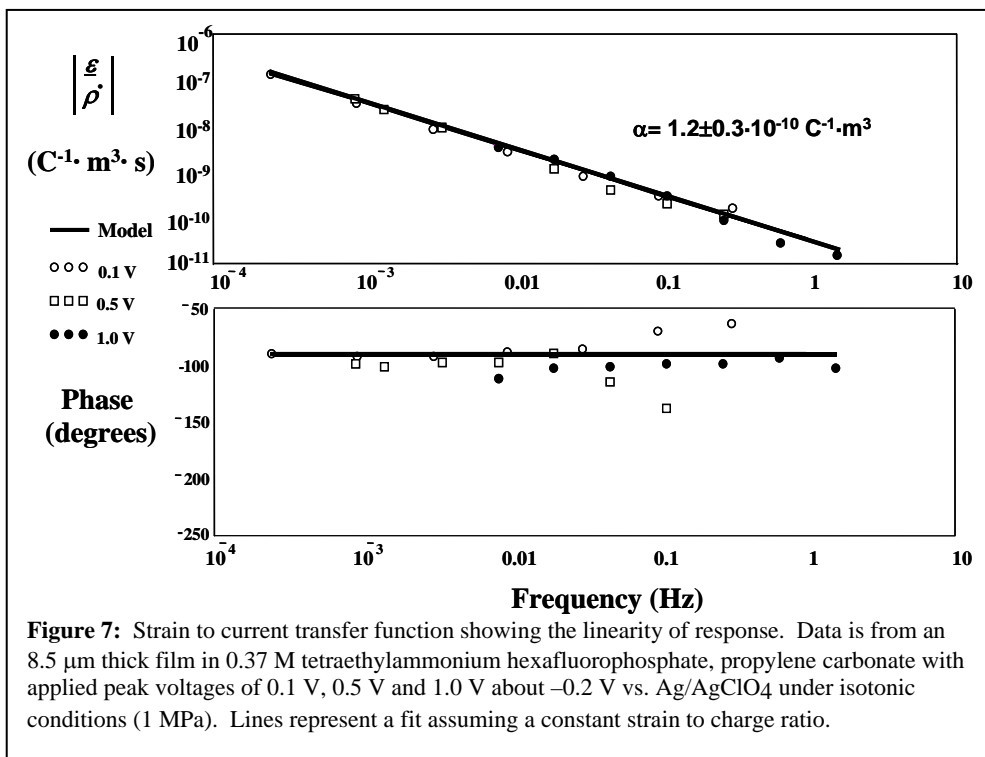


Figure 7: Strain to current transfer function showing the linearity of response. Data is from an $8.5 \mu\text{m}$ thick film in 0.37 M tetraethylammonium hexafluorophosphate, propylene carbonate with applied peak voltages of 0.1 V , 0.5 V and 1.0 V about -0.2 V vs. Ag/AgClO_4 under isotonic conditions (1 MPa). Lines represent a fit assuming a constant strain to charge ratio.

** End effects refer to reactions occurring at the ends of the polymer film where it is clamped, including reactions between the electrolyte and the stainless steel sheets that make electrical contact with the film.

thickness, following a diffusion model. Dissipation is minimized by operating at frequencies lower than the diffusion frequency, τ_D^{-1} and the RC charging frequency, τ_{RC}^{-1} .

6. ELECTROMECHANICAL PROPERTIES

A number of experimental results show that conducting polymer strain is proportional to charge^{1,5,9,10,14,16,43}. The relationship between strain, ε , stress, σ , charge density, ρ , and the stiffness, S is expressed

$$\varepsilon(s) = \alpha \cdot \rho(s) + \frac{\sigma(s)}{S(s)}, \quad (7)$$

where α is an empirically derived constant of proportionality referred to as the strain to charge ratio. The rightmost term describes the passive response, discussed in Section 4. Frequency response measurements are employed to determine the range of applied potentials, frequencies and loads over which Equation 7 is valid.

6.1. Strain to current transfer function

The strain to charge relationship is typically determined by applying steps in current under isotonic conditions (constant uniaxial load) and recording the resulting strain^{5,9,14,16,43}. An alternative is to measure strain in response to swept sine inputs. One advantage of the swept sine approach is that creep, as modeled by the right hand term in Equation 7, is filtered out. Rather than measure the strain to charge ratio, it is advantageous to measure the strain to current transfer function. Under isotonic conditions the strain to current transfer function is,

$$\frac{\varepsilon}{\dot{\rho}} = \frac{\alpha}{s}, \quad (8)$$

where $\dot{\rho}$ is the current per unit polymer volume.

Figure 7 shows the measured strain to current transfer function in a film held at 1 MPa for amplitudes of applied potential of up to ± 1 V. The response has the form of Equation 8, yielding a strain to charge ratio, $\alpha = 1.2 \pm 0.3 \cdot 10^{-10} \text{ m}^3 \cdot \text{C}^{-1}$. The strain amplitude at ± 1 V is 2.4 % at frequencies of 0.01 Hz and below, where the admittance is capacitive. At such low frequencies charge and voltage are directly proportional, as expressed by Equation 3. Strain and voltage may then be related,

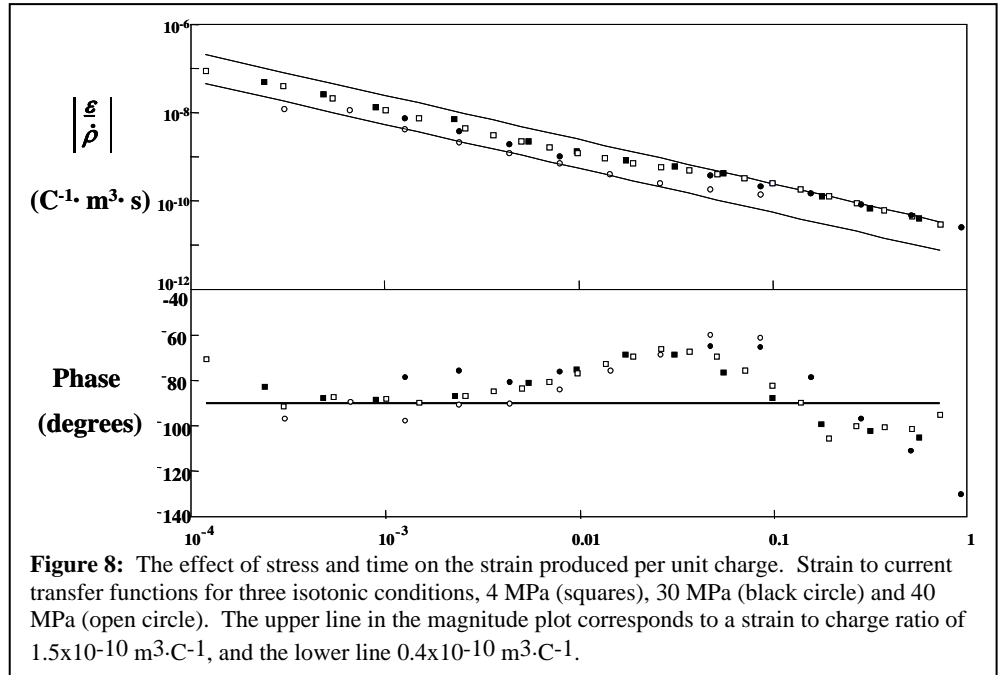


Figure 8: The effect of stress and time on the strain produced per unit charge. Strain to current transfer functions for three isotonic conditions, 4 MPa (squares), 30 MPa (black circle) and 40 MPa (open circle). The upper line in the magnitude plot corresponds to a strain to charge ratio of $1.5 \times 10^{-10} \text{ m}^3 \cdot \text{C}^{-1}$, and the lower line $0.4 \times 10^{-10} \text{ m}^3 \cdot \text{C}^{-1}$.

$$\varepsilon(s) = \alpha \cdot \frac{C_V}{V_p} \cdot V + \frac{\sigma(s)}{S(s)}, \quad (9)$$

where V_p is polymer volume. The strain to charge ratio was measured in 8.5 μm , 12.5 μm and 44 μm thick films¹⁰, and no significant differences were found. Significant changes in strain to charge are observed when larger potentials are applied. Recoverable strains reach 6 %, but large strains are achieved at the cost of visible polymer degradation¹⁰.

The application of loads greater than 4 MPa reveals a frequency dependence in the strain to charge ratio, as shown in Figure 8. The strain to charge ratio is unchanged from its lower load value at frequencies above 100 mHz. Below 100 mHz the strain to charge ratio drops, with the drop increasing with stress. At 34 MPa a 70 % drop in strain to charge ratio is

observed. The rise in phase above -90° signals dissipation. It appears that some molecular relaxation is occurring in response to the applied stresses, acting to reduce strain to charge.

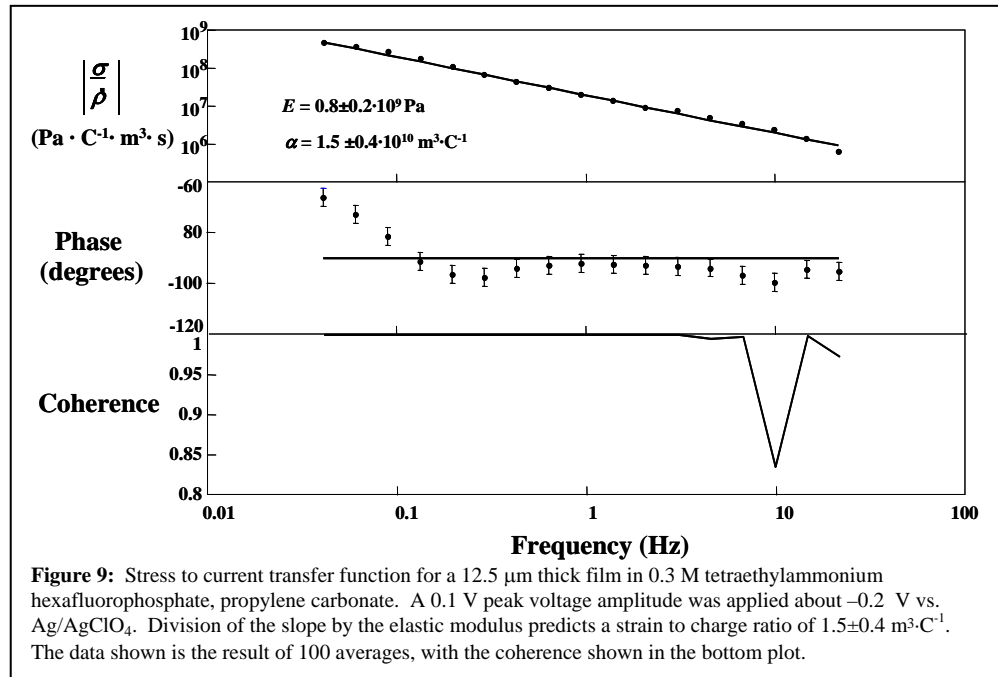


Figure 9: Stress to current transfer function for a 12.5 μm thick film in 0.3 M tetraethylammonium hexafluorophosphate, propylene carbonate. A 0.1 V peak voltage amplitude was applied about -0.2 V vs. Ag/AgClO_4 . Division of the slope by the elastic modulus predicts a strain to charge ratio of $1.5 \pm 0.4 \text{ m}^3 \cdot \text{C}^{-1}$. The data shown is the result of 100 averages, with the coherence shown in the bottom plot.

6.2. Stress to current transfer function

Given that strain is proportional to charge, Equation 7 anticipates that under isometric conditions stress, σ , will also be a function of charge transferred, via the relationship,

$$\frac{\sigma}{\dot{\rho}} = \frac{S \cdot \alpha}{s} \quad (10)$$

As confirmation, swept sine inputs are applied to polypyrrole films, and the stress to current transfer function is measured. The stress to charge ratio plotted in Figure 9 is from the same film

employed to obtain the strain to charge ratio in Figure 8. As expected, stress is proportional to charge. Division by the high frequency stress/strain transfer function of $S = E_f = 0.8 \text{ GPa}$, yields a strain to charge ratio estimate of $1.5 \pm 0.4 \text{ m}^3 \cdot \text{C}^{-1}$, which matches the $1.5 \pm 0.3 \text{ m}^3 \cdot \text{C}^{-1}$ estimated from the strain to current transfer function above 0.1 Hz in Figure 8. Note that, as with the strain to charge, the phase of the stress to charge ratio rises below 0.1 Hz, again suggesting a relaxation effect within the polymer.

6.3. Fast response

In bilayer actuators deflections are observed at frequencies in excess of 20 Hz^{7,8,14,17}. The force feedback mechanism used in measuring the strain to current transfer function does not have sufficient bandwidth to probe such frequencies. This limitation is avoided when measuring the stress to current transfer function, which is performed under isometric conditions. Figure 10 is a plot of the stress to current ratio from an 8.5 μm thick film. Note that variations in stress are observed at frequencies in excess of 30 Hz. At 30 Hz the RMS strain rate is $0.4 \text{ \%} \cdot \text{s}^{-1}$, and the strain amplitude is 0.007 %.

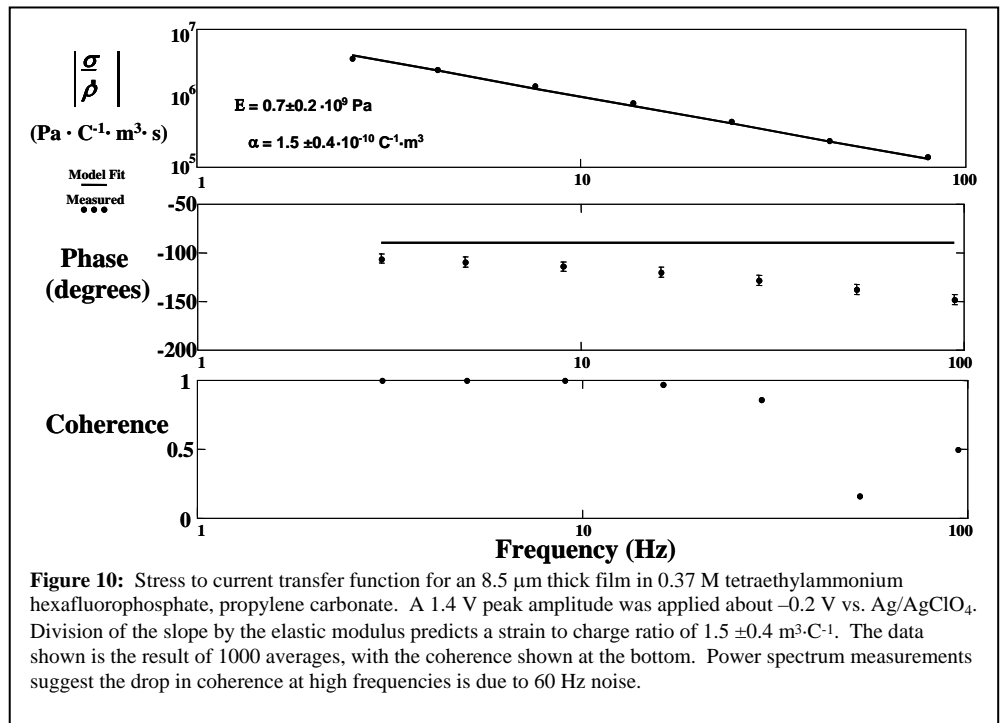


Figure 10: Stress to current transfer function for an 8.5 μm thick film in 0.37 M tetraethylammonium hexafluorophosphate, propylene carbonate. A 1.4 V peak amplitude was applied about -0.2 V vs. Ag/AgClO_4 . Division of the slope by the elastic modulus predicts a strain to charge ratio of $1.5 \pm 0.4 \text{ m}^3 \cdot \text{C}^{-1}$. The data shown is the result of 1000 averages, with the coherence shown at the bottom. Power spectrum measurements suggest the drop in coherence at high frequencies is due to 60 Hz noise.

6.4. Discussion and Summary

The strain to charge model fits the data effectively providing stresses are less than 4 MPa. The relationship is purely empirical, but its magnitude does suggest it is a function of ionic volume. Pei has observed that an insertion of charge will produce an expansion in polypyrrole, independent of whether the charge is positive or negative¹³. Interestingly, in the case of hexafluorophosphate doping of polypyrrole in propylene carbonate, each added charge appears to stretch the polymer by its own volume^{††}. This suggests that the ions squeeze into the polymer, pushing polymer and solvent aside, and generating strain. The strain to charge ratio doubles to $3 \times 10^{-10} \text{ m}^3 \cdot \text{C}^{-1}$ in aqueous tetraethylammonium hexafluorophosphate electrolytes¹⁰. It is speculated that hexafluorophosphate ions entrain water molecules when entering polypyrrole from an aqueous solution, thereby explaining the additional displacement.

7. ELECTROMECHANICAL EFFICIENCY.

The efficiency of electrical to mechanical energy conversion, e , is

$$e = \frac{\int F \cdot dx}{\int V \cdot dQ} = \frac{\int \sigma \cdot d\varepsilon}{\int V \cdot d\rho}, \quad (11)$$

where F is force, x is displacement, V is applied voltage, Q is charge, σ is stress, ε is strain, ρ is charge density and integration is taken over a complete cycle. Ideally a large fraction of the input energy is output as work. Unfortunately this is not the case for polypyrrole. However, since most of the input electrical energy is stored, recovering or reusing this energy greatly improves efficiency.

7.1. Efficiency of step potential input under isotonic conditions

The factors influencing efficiency are described by exploring the case of a step voltage input, V , applied to a polymer under constant uniaxial load, σ . In the case of a constant load, σ , and a step in applied voltage, the modeled efficiency is,

$$e = \frac{\int \sigma \cdot \alpha \cdot d\rho}{\int V \cdot d\rho} = \frac{\sigma \cdot \alpha \cdot \int d\rho}{V \cdot \int d\rho} = \frac{\sigma \cdot \alpha}{V}, \quad (12)$$

providing that no stored electrical energy is recovered. Increasing load and the strain to charge ratio, and decreasing the applied potential, maximize efficiency. Currently it is impractical to employ loads exceeding 4 MPa because creep becomes significant and the strain to charge ratio is time dependent. Given an applied stress of 4 MPa and the measured $\alpha = 1.5 \times 10^{-10} \text{ m}^3 \cdot \text{C}^{-1}$, the numerator is 0.6 mV. The application of a voltage amplitude $V = \pm 0.6 \text{ V}$ produces a strain of $\pm 0.7 \%$, as calculated using Equation 9 with $C_V V^l = 8 \times 10^7 \text{ F} \cdot \text{m}^{-3}$. The efficiency is 0.1 %. The highest efficiency measured from the frequency response data is 3 % without electrical energy recovery and 7 % assuming all stored energy is recovered¹⁰. However, these values are obtained over short timescales at an activation voltage of 0.1 V, corresponding to a strain of 0.1 %, and a stress of 30 MPa. Very high efficiencies can be obtained by employing low voltages, but this is done at the expense of strain.

7.2. Improving Efficiency

The small magnitude of electromechanical coupling in polypyrrole will require one or more strategies if high efficiencies are to be obtained. One approach is to recover electrical energy stored in the polymer. In order to achieve efficiencies above 10 % while maintaining large strains (>1%) and not exceeding 4 MPa in load the recovery of close to 99 % of the input energy is necessary. Figure 6 shows that at low frequencies polypyrrole acts as a capacitor, storing up to 92 % of the input energy. The recovery of 99 % of input energy will require careful elimination of loss mechanisms, and very efficient energy recovery or resonant circuitry. An alternative is to process the polymer such that the threshold load is increased. This might be achieved by stretch alignment, which can lead to fibers having tensile strengths in excess of 400 GPa, and much reduced creep levels¹. The drawback of this procedure is that the strain to charge ratio is likely reduced during the alignment process⁵. Yet another approach is to increase the strain to charge ratio without severely sacrificing the load bearing

^{††} This calculation assumes isotropic expansion and small strains. The volume change per unit charge, $\Delta v = 3 \cdot \alpha \cdot e$, where e is the fundamental charge. Then $\Delta v = 0.07 \text{ nm}^3/\text{charge}$, which is within 30 % of the volume of PF_6^- , as determined from CambridgeSoft's Chem3D Pro Version 4.0, www.chemoffice.com.

characteristics. In order to be effective, this may involve redesign at the molecular level⁴⁴. Finally, one may choose to be content with small strains, $\ll 1\%$, where efficiencies are moderate to high⁴⁵.

7.3. Summary

Electromechanical coupling in polypyrrole is small, leading to low efficiencies. If high efficiencies and large strains are desired most of the input energy will need to be recovered. An alternative is to investigate new materials that promise to provide more work for a given charge.

8. DISCUSSION AND CONCLUSION

The properties of hexafluorophosphate doped conducting polymers, including synthesis conditions, stress-strain relationships, electrochemistry and electromechanical coupling have been summarized. Equations 1,2,4 and 7 together describe the relationship between voltage, current, load and displacement. The modeling enables the designer to optimize actuator geometry for target loads, displacements, velocities, powers, and efficiencies. Further work is required to recognize the nature of loss mechanisms in polypyrrole, and determine limits on cycle life.

ACKNOWLEDGEMENTS

This work is partially supported by the Office of Naval Research and General Motors. Many thanks to Patrick Anquetil and Ann Madden for their valuable comments.

REFERENCE LIST

1. R. H. Baughman, R. L. Shacklette, R. L. Elsenbaumer, "Micro Electromechanical Actuators based on Conducting Polymers", *Topics in Molecular Organization and Engineering: Molecular Electronics*, P. I. Lazarev, Ed., vol. 7, pp.267, Kluwer, Dordrecht, 1991.
2. M. R. Gandhi, P. Murray, G. M. Spinks, G. G. Wallace, "Mechanism of Electromechanical Actuation in Polypyrrole", *Synthetic Metals* **73**, pp. 247-256, 1995.
3. Q. Pei and O. Ingnas, "Electrochemical Application of the Bending Beam Method. 1. Mass Transport and Volume Changes in Polypyrrole During Redox.", *Journal of Physical Chemistry* **96**, pp. 10507-10514, 1992.
4. E. Smela, O. Ingnas, I. Lundstrom, "Controlled Folding of Micrometer-Size Structures", *Science* **268**, pp. 1735-1738, 1995.
5. T. E. Herod and J. B. Schlenoff, "Doping Induced Strain in Polyaniline: Stretchoelectrochemistry", *Chemistry of Materials* **5**, pp. 951-955, 1993.
6. T. F. Otero, J. Rodriguez, E. Angulo, C. Santamaria, "Artificial Muscles From Bilayer Structures", *Synthetic Metals* **55-57**, pp. 3713-3717, 1993.
7. K. Kaneto, M. Kaneko, Y. Min, A. G. MacDiarmid, ""Artificial Muscle" : Electromechanical Actuators Using Polyaniline Films", *Synthetic Metals* **71**, pp. 2211-2212, 1995.
8. Madden, J. D., Lafontaine, S. R., and Hunter, I. W., "Fabrication by Electrodeposition: Building 3D Structures and Polymer Actuators", *Proceedings - Micro Machine and Human Science* **95**, Nagoya, Japan, 1995.
9. A. Mazzoldi, A. Della Santa, D. De Rossi, "Conducting polymer actuators: Properties and modeling", *Polymer Sensors and Actuators*, Y. Osada and D. E. De Rossi, Eds., Springer Verlag, Heidelberg, 1999.
10. J. D. Madden, "Conducting Polymer Actuators", *Ph.D. Thesis*, Massachusetts Institute of Technology, Cambridge, MA, 2000.
11. T. A. Skotheim, R. L. Elsenbaumer, J. R. Reynolds, *Handbook of Conducting Polymers*, 2nd ed., Marcel Dekker, New York, 1998.
12. E. T. Jones, E. Chao, M. J. Wrighton, "Preparation and Characterization of Molecule-Based Transistors With a 50 Nm Separation", *Journal of the American Chemical Society* **109**, pp. 5526-5529, 1987.
13. Q. Pei and O. Ingnas, "Electrochemical Applications of the Beam Bending Method; a Novel Way to Study Ion Transport in Electroactive Polymers", *Solid State Ionics* **60**, pp. 161-166, 1993.
14. J. D. Madden, C. J. Brennan, J. Dubow, "Progress Towards An Automatic, Microfabricated Polymer Air -Fluid Sampling Inlet", *Accession Number AD-A332 030/6/XAB*, NTIS, Springfield,VA, 1997.
15. A. Della Santa, D. De Rossi, A. Mazzoldi, "Performance and Work Capacity of Polypyrrole Conducting Polymer Linear Actuator", *Synthetic Metals* **90**, pp. 93-100, 1997.
16. J. D. Madden, R. A. Cush, T. S. Kanigan, C. J. Brennan, I. W. Hunter, "Encapsulated Polypyrrole Actuators", *Synthetic Metals* **105**, pp. 61-64, 1999.

⁴⁴ Equation 12, the right hand side of which is empirically derived, predicts that efficiency can exceed 1 at sub-millivolt potentials. A modified equation has been proposed which includes mechanical to electrical coupling¹⁰.

17. J. D. Madden, R. A. Cush, T. S. Kanigan, I. W. Hunter, "Fast Contracting Polypyrrole Actuators", *Synthetic Metals* **113**, pp. 185-193, 2000.
18. E. W. H. Jager, E. Smela, O. Ingnas, "Microfabricating Conjugated Polymer Actuators", *Science* **290**, pp. 1540-1545, 2000.
19. Hunter, I. W. and Lafontaine, S., "A comparison of muscle with artificial actuators", *Technical Digest IEEE Solid State Sensors and Actuators Workshop*, pp. 178-185, IEEE, 1992.
20. R. H. Baughman, "Conducting Polymer Artificial Muscles", *Synthetic Metals* **78**, pp. 339-353, 1996.
21. T. F. Otero, "Artificial Muscles, electrodisolutoin and redox processes in conducting polymers", *Handbook of organic and conductive molecules and polymers*, H. S. Nalwa, Ed., vol. 4, pp.517-594, John Wiley & Sons, Chichester, 1997.
22. M. Yamaura, T. Hagiwara, K. Iwata, "Enhancement of Electrical Conductivity of Polypyrrole Film by Stretching: Counter Ion Effect", *Synthetic Metals* **26**, pp. 209-224, 1988.
23. A. S. Hutchison, T. W. Lewis, S. E. Moulton, G. M. Spinks, G. G. Wallace, "Development of Polypyrrole-Based Electromechanical Actuators", *Synthetic Metals* **113**, pp. 121-127, 2000.
24. Q. Pei and O. Ingnas, "Conjugated Polymers and the Bending Cantilever Method: Electrical Muscles and Smart Devices", *Advanced Materials* **4**, pp. 277-278, 1992.
25. E. Smela, O. Ingnas, Q. Pei, I. Lundstrom, "Electrochemical Muscles: Micromachining Fingers and Corkscrews", *Advanced Materials* **5**, pp. 630-632, 1993.
26. Y.-J. Lee, "X-ray Diffraction Studies of Polypyrrole", *MIT Materials Science and Engineering Undergraduate Thesis*, Cambridge, MA, 1999.
27. Y. Nogami, J.-P. Pouget, T. Ishiguro, "Structure of Highly Conducting PF₆⁻-Doped Polypyrrole", *Synthetic Metals* **62**, pp. 257-263, 1994.
28. J. P. Pouget et al., "Recent Structural Investigations of Metallic Polymers", *Synthetic Metals* **65**, pp. 131-140, 1994.
29. R. S. Kohlman and A. J. Epstein, "Insulator-metal transition and inhomogeneous metallic state in conducting polymers", *Handbook of Conducting Polymers*, T. A. Skotheim, R. L. Elsenbaumer, J. R. Reynolds, Eds., pp.85-122, Marcel Dekker, New York, 1998.
30. M. Yamaura, K. Sato, K. Iwata, "Memory Effect of Electrical Conductivity Upon the Counter-Anion Exchange of Polypyrrole Films", *Synthetic Metals* **48**, pp. 337-354, 1992.
31. M. Yamaura, K. Sato, T. Hagiwara, "Effect of Counter-Anion Exchange on Electrical Conductivity of Polypyrrole Films", *Synthetic Metals* **39**, pp. 43-60, 1990.
32. K. Sato, M. Yamaura, T. Hagiwara, "Study on the Electrical Conduction Mechanism of Polypyrrole Films", *Synthetic Metals* **40**, pp. 35-48, 1991.
33. J. Courtot-Coupez and M. L'Her, "Electrochimie Dans La Carbonate De Propylene. II. - Domaine D'Electroactivite Et L'Influence De L'Eau.", *Bulletin de la societe chimique de France* **4**, pp. 1631-1636, 1970.
34. B. J. Feldman, P. Burgmayer, R. W. Murray, "The Potential Dependence of Electrical Conductivity and Chemical Charge Storage of Poly(Pyrrole) Films on Electrodes", *Journal of the American Chemical Society* **107**, pp. 872-878, 1985.
35. R. A. Bull, F.-R. F. Fan, A. J. Bard, "Polymer Films on Electrodes", *Journal of the Electrochemical Society* **129**, pp. 1009-1015, 1982.
36. H. Mao, J. Ochmanska, C. D. Paulse, P. G. Pickup, "Ion Transport in Pyrrole-Based Polymer Films", *Faraday Discussions of the Chemical Society* **88**, pp. 165-176, 1989.
37. T. Amemiya, K. Hashimoto, A. Fujishima, "Frequency-Resolved Faradaic Processes in Polypyrrole Films Observed by Electromodulation Techniques: Electrochemical Impedance and Color Impedance Spectroscopies", *Journal of Physical Chemistry* **97**, pp. 4187-4191, 1993.
38. R. M. Penner and C. R. Martin, "Electrochemical Investigations of Electronically Conductive Polymers. 2. Evaluation of Charge-Transport Rates in Polypyrrole Using an Alternating Current Impedance Method.", *Journal of Physical Chemistry* **93**, pp. 984-989, 1989.
39. A. J. Bard and L. R. Faulkner, *Electrochemical Methods, Fundamentals and Applications*, Wiley, New York, 1980.
40. M. Kalaji, L. M. Peter, L. M. Abrantes, J. C. Mesquita, "Microelectrode Studies of Fast Switching in Polyaniline Films", *Journal of electroanalytical chemistry* **274**, pp. 289-295, 1989.
41. J. C. Lacroix, K. K. Kanazawa, A. Diaz, "Polyaniline: A Very Fast Electrochromic Material", *Journal of the electrochemical society* **136**, pp. 1308-1313, 1989.
42. E. W. H. Jager, E. Smela, O. Ingnas, "On-Chip Microelectrodes for Electrochemistry With Moveable PPy Bilayer Actuators As Working Electrodes", *Sensors and Actuators B* **56**, pp. 73-78, 1999.
43. M. Kaneko, M. Fukui, W. Takashima, K. Kaneto, " Electrolyte and Strain Dependences of Chemomechanical Deformation of Polyaniline Film", *Synthetic Metals* **84**, pp. 795-796, 1997.
44. J. D. Madden, H.-H. Yu, P. A. Anquetil, T. M. Swager, I. W. Hunter, "Large Strain Molecular Actuators", *EAP Newsletter* **2**, pp. 9-10, 2000.